



## Research article

# Potential use of polydimethylsiloxane phantom in acupuncture manipulation practice

Yeonsun Lee<sup>a</sup>, Hyosang Lee<sup>b</sup>, Eun Jung Kim<sup>c</sup>, Seung Deok Lee<sup>d</sup>, Chan Yung Jung<sup>e,1,\*</sup>

<sup>a</sup> Department of Acupuncture & Moxibustion, Bucheon Jaseng Hospital of Oriental Medicine, Bucheon, 14598, Republic of Korea

<sup>b</sup> Haptic intelligence Department, Max Planck Institute for Intelligent Systems, Stuttgart 70569, Germany

<sup>c</sup> Department of Acupuncture & Moxibustion, Dongguk University Bundang Oriental Hospital, Seongnam, 13601, Republic of Korea

<sup>d</sup> Dongguk University Los Angeles, 440 Shatto Pl, Los Angeles, CA 90020, USA

<sup>e</sup> Department of Acupuncture & Moxibustion, Dongguk University Ilsan Oriental Hospital, Goyang, 10326, Republic of Korea

## ARTICLE INFO

## Keywords:

Acupuncture needle

Friction force

Karnopp friction

Tissue-mimicking phantom

Acupuncture manipulation

## ABSTRACT

**Objectives:** Sufficient trials of acupuncture manipulations should be practiced to obtain proficiency. However, there is not an adequate quantitative methodology for selecting a tissue-mimicking phantom that effectively reproduces the mechanical behavior that occurs during acupuncture. The objective of this study was to determine the proper mixing ratio of polydimethylsiloxane (PDMS) to obtain tissue phantom that is the most similar to porcine phantoms. **Design:** An automatic needle manipulator equipped with a six-degrees-of-freedom force/torque sensor was installed to monitor the interaction force that occurred when the acupuncture needle performed lifting–thrusting and twirling manipulations. Four types of PDMS phantoms, composed of two silicone elastomers with different hardener ratios, were studied alongside four control groups consisting of different porcine sites. A Visual Analog Scale was used to quantify the similarity of the PDMS phantoms to the controls by 11 Korean medical doctors.

**Results:** Using the lifting–thrusting method, PDMS D (mixing ratio of 1:4.5) and control 2 (porcine blade shoulder) revealed no significant difference in the dynamic friction coefficients or maximum and minimum friction force values ( $P < 0.001$ ). Using the twirling method, PDMS D showed no significant difference from all controls in the viscosity coefficient or maximum and minimum torque values ( $P \leq 0.001$ ). By practitioners, PDMS D showed the greatest score.

**Conclusion:** PDMS D delivered a haptic sensation that is most similar to that of biological tissues in the case of acu-needle lifting–thrusting and twirling methods. This finding guides the preparation of tissue phantoms for acu-needle studies and acupuncture training.

## 1. Introduction

In acupuncture therapy, manipulating and inserting an acupuncture needle (acu-needle) creates a mechanical stimulation that affects treatment outcomes [1]. The main acu-needle manipulation consists of the insertion and coaxial rotation along the needle. These movements stimulate physical acu-needle sensations in the patient [2,3]. The acu-needle operator generally judges the

\* Corresponding author.

E-mail address: [yyoung81@hanmail.net](mailto:yyoung81@hanmail.net) (C.Y. Jung).

<sup>1</sup> Present address: Yeonsu-gu Public Health Center, Incheon, 21915, Republic of Korea.

<https://doi.org/10.1016/j.heliyon.2024.e25428>

Received 14 August 2022; Received in revised form 14 January 2024; Accepted 26 January 2024

Available online 27 January 2024

2405-8440/© 2024 Published by Elsevier Ltd.

This is an open access article under the CC BY-NC-ND license

(<http://creativecommons.org/licenses/by-nc-nd/4.0/>).

### Abbreviations

RTV	Room-Temperature-Vulcanizing
SAS	Statistical Analysis System software
VAS	Visual Analogue Scale
PDMS	Polydimethylsiloxane
CON	Control

appropriateness of the stimulation through the operator's tactile sensation and the patient's reaction [4,5]. This subtle manipulation technique is learned through practice using tissue-mimicking phantoms instead of human skin. Through simulation training, students can improve their accuracy in practical examinations [6].

Tissue-mimicking phantoms are widely used in medicine to test robotic surgery systems [7] or perform ultrasound-guided biopsy [8]. Polydimethylsiloxane (PDMS) composed of silicone is commonly used as a phantom due to its noncytotoxic, nonflammable, and biocompatible features [9–11]. Although several studies have revealed that quantitative forces are generated from the needle-tissue interaction [4,5,12], including those that used PDMS as a tissue-mimicking phantom [13,14], acu-needles are different from regular injection needles in terms of incision shape of the needle tip, needle thickness, and elasticity. In Jang et al. [15]'s survey on acupoint locating training and needling training using the phantom model, only two papers [16,17] used silicone phantoms for both training sessions. In order to practice acupuncture effectively, various manipulations are required, along with the use of a phantom model that accurately reflects different human tissues.

In preliminary acupuncture studies, various raw materials, such as paper, cotton, cucumbers, and apples, have been used as a tissue-mimicking phantom [18]. However, those materials were not suitable for reproducing the mechanical behavior of the lifting–thrusting manipulation. In addition, Lee et al. [12] suggested agarose gel as an alternative phantom, but the practical application of this substance is limited by its short shelf life and the fact it does not reflect the full range of acupuncture points of the human body. On the other hand, while PDMS can vary depending on the type, it can also have a longer aging period depending on the mixing ratio and the curing temperature [19]. Additionally, it possesses the characteristic of being able to configure physical properties at various rates [10].

To evaluate phantoms, Son et al. [5] quantitatively compared acu-needle movements using an interaction force and coefficient. The force reflects the amount of acupuncture sensation felt by the operator when performing manipulations, which was intended to be quantified using the coefficient. In this method, the degree of sensation can be compared by measuring the coefficient of friction occurring during two basic manipulation methods: lifting–thrusting and twirling.

The main purpose of this study was to determine the proper mixing ratio of two silicone elastomers for PDMS tissue phantom that is the most similar to porcine phantoms. The PDMS tissue phantom was quantitatively evaluated by an automatic needle manipulator and was qualitatively validated by experts. The quantitative evaluation is done by comparing friction coefficients during the lifting–thrusting and twirling manipulation methods. Eleven Korean medical doctors who performed acu-needle manipulation on each phantom evaluated the similarity between the tissue phantom and real human tissue; the acu-needle sensation was evaluated using VAS (Visual Analogue Scale).

## 2. Materials and methods

### 2.1. Experimental Setup

A machine maneuvering a needle at a constant amplitude and frequency was designed to reproduce acupuncture manipulation (Fig. 1). An acu-needle was directly connected to a 6-axis force/torque sensor to measure the reaction force/torque that resulted in response to the needle's movement. The motor was based on Simulink (MathWorks Inc., USA) and Quarc (QUANSER, Canada)

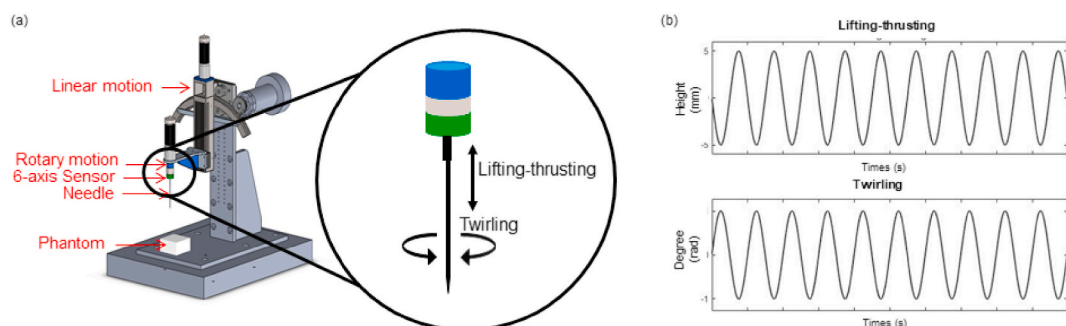


Fig. 1. Image (a) and movements of equipment used, and the expected motion graph (b).

programs and was operated on analog voltage through an automatic driver in an external control box (QUANSER, Canada). The machine was capable of vertical, linear, and rotary motions, but in this study, only linear and rotary motion were used to reproduce the lifting–thrusting and twirling acupuncture methods, respectively.

## 2.2. Tissue phantoms

### 2.2.1. Polydimethylsiloxane

Silbione® Room-Temperature-Vulcanizing (RTV) 4420 QC (Elkem Silicones, France) was used as a tissue-mimicking phantom. Polydimethylsiloxane is produced at room temperature (22°C–24 °C) by mixing two silicone elastomers: referred to as A and B, respectively, in this study. The mixing ratios of the two silicone elastomers were 1:3 (PDMS A), 1:3.5 (PDMS B), 1:4 (PDMS C), and 1:4.5 (PDMS D). During the curing process, air bubbles were minimized as much as possible by removing air through the vacuum pump (Woosung Vacuum CO., LTD, Korea). The elastomer mixture was poured into a mold (5 cm length × 5 cm width × 3 cm height measured as cubic centimeters [cm<sup>3</sup>]) and cured until it was sufficiently hardened.

### 2.2.2. Control phantom

The control group used porcine phantoms to represent a human body [20–22]. These porcine phantoms were prepared within ten days of death in the form of porcine shank (Control 1, CON 1), blade shoulder (Control 2, CON 2), picnic (Control 3, CON 3), and belly (Control 4, CON 4). As acupuncture can be applied to various parts of the human body, such as the upper limbs, lower limbs, and abdomen, several porcine parts were selected to reflect this.

## 2.3. Acu-needle manipulation techniques

Lifting–thrusting and twirling methods are widely used acu-needle manipulation techniques. These are basic manipulation techniques that move, hasten, supplement, and drain  $qi$  [23,24]. The lifting–thrusting method involves inserting and extracting an acu-needle. In this study, a sinusoidal motion with an amplitude of 5 mm and a frequency of 1 Hz [25] was activated. The twirling method involves rotating an acu-needle after it has been inserted. In this study, a sinusoidal motion with an amplitude of  $\pi$  radian and frequency of 0.2 Hz was used [26].

## 2.4. Estimating friction coefficients

Friction coefficients are estimated using the modified Karnopp friction model introduced by Okamura et al. [27]. In this model, the interaction force measured at the needle base consists of three factors.

$$F_{measured} = F_{stiffness} + F_{friction} + F_{cutting} \quad (1)$$

where  $F_{measured}$  is the value measured through the experiment;  $F_{stiffness}$  is associated with the stiffness of the phantom and the force generated by the elasticity of the soft tissue;  $F_{friction}$  refers to the friction force generated along the needle surface; and  $F_{cutting}$  represents the cutting force that occurs at the needle when the needle penetrates soft tissue.

In this study, lifting–thrusting and twirling manipulation methods were evaluated. Since the acu-needle only moves along the axial direction, the  $F_{stiffness}$  is assumed to be zero. In addition, the first needle insertion process was excluded because acu-needle stimulation targets the movement after the needle is inserted. Therefore,  $F_{cutting}$  is also assumed to be zero.  $F_{friction}$  is applied to the modified Karnopp friction model (Equations (2) and (3)).

When the needle is moving with acceleration,  $F_{measured}$  includes the force caused by the inertia of the acu-needle ( $F_{inertia}$ ). In this sense, Equation (1) can be modified as follows.

$$F_{measured} = F_{inertia} + F_{friction} \quad (2)$$

$$F_{measured} = ma + F_{friction} \quad (3)$$

where  $m$  is the mass of the acupuncture needle, and  $a$  is the acceleration of the acupuncture needle. For the lifting–thrusting method, the modified Karnopp friction model was applied to estimate the dynamic friction and static friction coefficients, as shown in Equation (4). This model formulates the relationship between the friction force and the relative velocity of the acu-needle and tissue phantom. The dynamic friction force is calculated from the measured force, assuming the constant contact area after the acu-needle is inserted.

$$F_{friction} = F_{measured} - ma = l(C_p \text{sgn}(v_p) + b_p v_p + C_n \text{sgn}(v_n) + b_n v_n) \quad (4)$$

where  $l$  is the contact length of the phantom and the acupuncture needle;  $C_n$  and  $C_p$  are the negative and positive coefficients of dynamic friction, respectively;  $b_n$  and  $b_p$  are the negative and positive coefficients of viscosity, respectively;  $v_n$  and  $v_p$  are the relative velocities of the tissue with the acu-needle according to the insertion direction, respectively; and  $\text{sgn}$  is the signum function.

Since the mass, acceleration, and relative velocity of the acupuncture needle were measured through the experiment,  $C_p$ ,  $C_n$ ,  $b_p$ , and  $b_n$  can be obtained using the least-squares method. The static friction forces  $D_n$  and  $D_p$  are calculated at the moment when the relative velocity is zero, meaning that lifting and thrusting change.

In the case of twirling, Reed et al.'s equation [28] was applied, as shown in Equation (5). The measured force is modeled as the force

generated by the angular velocity of the needle:

$$T_{\pi} = \beta \times \dot{\theta} \tag{5}$$

where  $\beta$  is the rotational viscosity coefficient, and  $\dot{\theta}$  is the angular velocity of the radian. This assumes that the viscosity of the tissue only relates to the interaction between the acu-needle and tissue, and the torque at a particular angle of rotation during a constant motion is only affected by damping. In this study, the viscosity coefficient was calculated at a rotation angle of the  $\pi$  radian, where

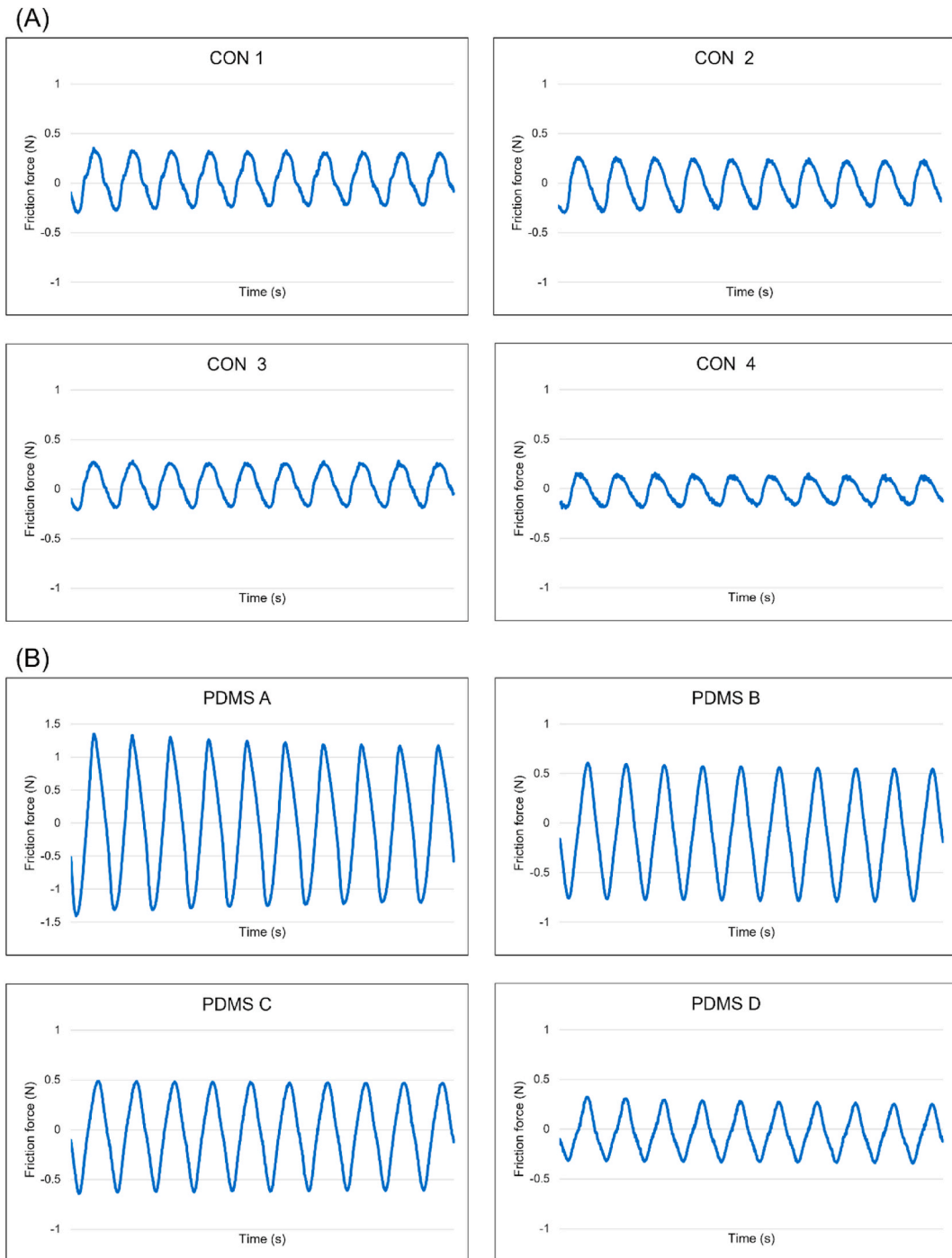


**Fig. 2.** Change in friction force over time for control phantoms (A) and polydimethylsiloxane phantoms (B) during lifting-thrusting (CON: control phantoms; PDMS: polydimethylsiloxane phantoms).

constant angular velocity is formed [4].

2.5. Statistical analysis

Statistical analysis was performed using a Statistical Analysis System software (SAS Institute Inc., USA). The coefficients ( $C_p$ ,  $C_n$ ,  $D_p$ ,  $D_n$ ,  $b_p$ ,  $b_n$ , and  $\beta$ ) were calculated from the control group, and the PDMS phantom was analyzed using one-way analysis of variance. Additionally, Tukey’s honestly significant difference test was performed, with  $P < 0.05$  considered to be statistically significant.

2.6. Qualitative validation from experts

Eleven Korean medicine doctors were recruited to evaluate the tissue phantoms located in a blind box. The doctors inserted an acupuncture needle into the PDMS A, B, C, and D, and control phantoms to a depth of 15 mm [18,29]. Then, using the visual analysis scale (VAS), they evaluated the similarity, which was measured on a scale of 0–100.

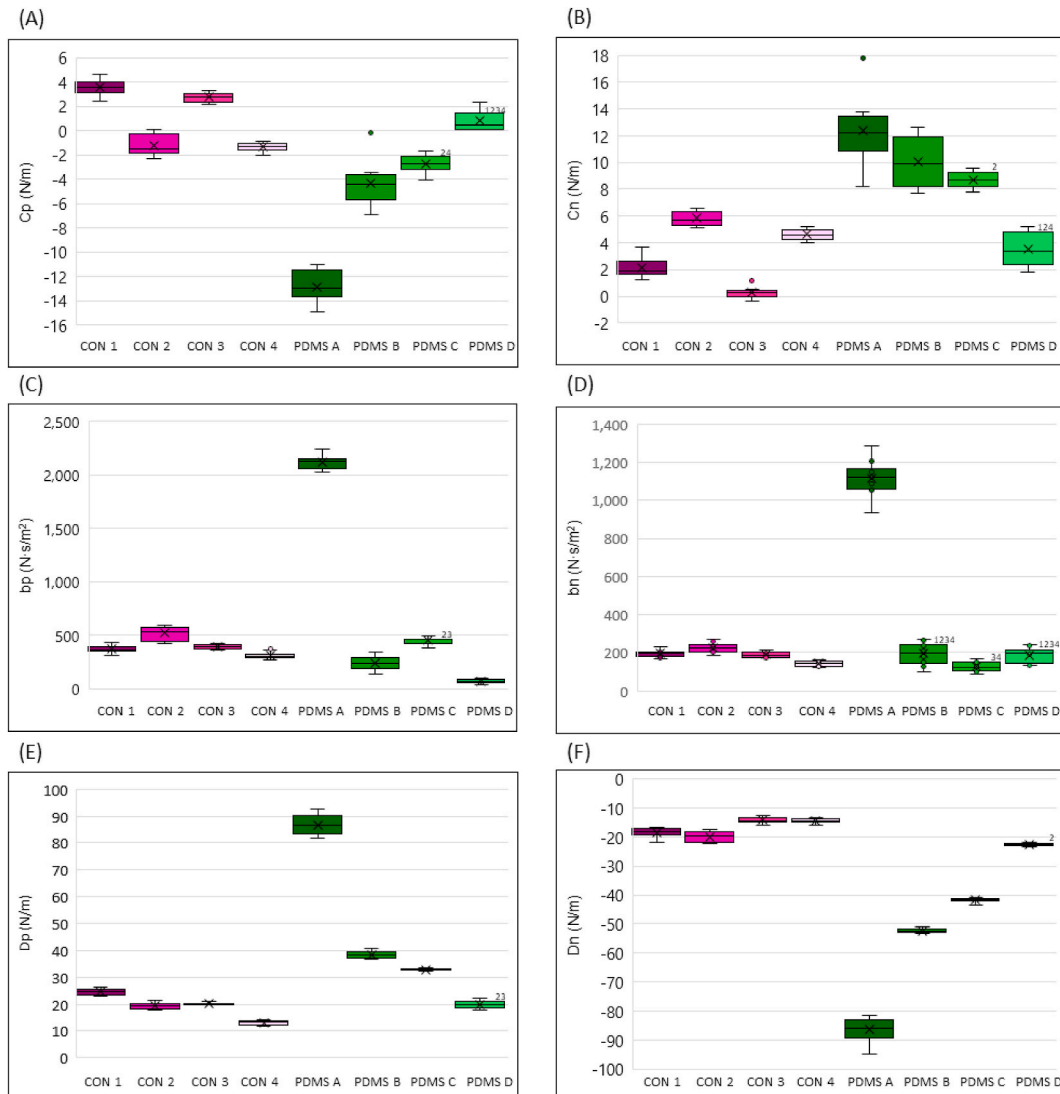


**Fig. 3.** Friction coefficients for each phantom during lifting–thrusting with the numbers referring to CON that do not differ significantly from PDMS. (CON: control phantom; PDMS: polydimethylsiloxane phantom;  $C_p$ : positive dynamic friction coefficient;  $C_n$ : negative dynamic friction coefficient;  $b_p$ : positive viscosity coefficient;  $b_n$ : negative viscosity coefficient;  $D_p$ : positive static friction coefficient;  $D_n$ : negative static friction coefficient)  $P < 0.05$ .

### 3. Results

#### 3.1. Lifting–thrusting experiments

Using the automatic needle manipulator, the acu-needle was inserted to a depth of 15 mm, and a sinusoidal motion of 5 mm amplitude and 1 Hz frequency was performed. The change in force over time that occurs when the acu-needle moves is shown in Fig. 2. Fig. 2(A) represents values from CON 1 to 4, while Fig. 2(B) represents values from PDMS A to D. PDMS D showed a similar range of values to the control phantoms.

Fig. 3(A–F) represent the coefficients obtained through the lifting–thrusting method. When comparing the values of  $C_p$  as shown in Fig. 3(A), which have been used as a criterion for evaluating acu-needle sensations in linear motion [5], PDMS A and PDMS B showed large values; there was a significant difference between the controls; and there was no similarity in the values. On the other hand, PDMS C was not significantly different from CON 2 and CON 4, and PDMS D was not significantly different from any of the controls. From these results, we can see that PDMS A and PDMS B are not appropriate to use as tissue-mimicking phantoms.

To compare the differences between PDMS C and PDMS D, the maximum and minimum values of the force generated in a single exercise were calculated and are listed in Table 1. This was compared because the magnitude of the force generated during exercise is the magnitude of the force generated between the acu-needle and the tissue, and this is the absolute amount of physical stimulation by the acu-needle.

The results showed that the larger the component ratio of PDMS, the smaller the friction force values. At the maximum value, there were no PDMS phantoms that had similar values to CON 1 or CON 4. PDMS D was not statistically significantly different from CON 2 and CON 3. At the minimum value, statistical analysis showed only PDMS D and CON 2 were not significantly different. Through the experiment, it was discovered that among the four selected tissue-mimicking phantoms, PDMS D showed the greatest similarity to CON 2 in terms of  $C_p$  and maximum and minimum friction force values. This means that PDMS D can be used as a phantom to practice lifting–thrusting techniques in place of CON 2.

The closer the two silicone elastomers of PDMS are to a ratio of 1:4.5, the more the positive dynamic friction coefficient of the acu-needle sensation, which then achieves a sensation that is most similar to porcine phantoms. For a more detailed comparison, when all friction coefficients were compared, PDMS D was not statistically significantly different from the six friction coefficients calculated for CON 2.

Fig. 4(A–D) are the comparison of CON 1 to 4 and PDMS A to D, respectively. In the VAS test results, PDMS D was evaluated with the highest score (>71.42 mm), so, of the four PDMSs, it was considered to be the most similar to each of the controls.

#### 3.2. Twirling experiments

The rotary motion was a sine wave with an amplitude of  $\pi$  radian and a frequency of 0.2 Hz after the acu-needle was inserted 15 mm into the phantom. Fig. 5 shows the change of torque overtime during the rotary motion of the acu-needle. Fig. 5(A) shows the values for CON 1 to 4, while Fig. 5(B) displays the values for PDMS A to D.

The viscosity coefficient,  $\beta$ , is analyzed as a criterion for determining acu-needle sensation during the rotary motion [4]. As a result, PDMS A, PDMS B, and PDMS C significantly differed from each of the controls. Only PDMS D did not differ significantly from any of the controls. This result indicates that PDMS A, PDMS B, and PDMS C are not appropriate as tissue-mimicking phantoms.

**Table 1**  
Friction force of the lifting–thrusting experiments for Control and Polydimethylsiloxane phantoms.

	(N)					ANOVA p-value	Tukey’s HSD	
		PDMS A <sup>a</sup>		PDMS B <sup>f</sup>				
		mean ± SD	mean ± SD	mean ± SD	mean ± SD			
CON 1 <sup>a</sup> mean ± SD	Max	0.37 ± 0.07	1.30 ± 0.32	0.58 ± 0.11	0.49 ± 0.06	0.30 ± 0.05	<0.001	–
	Min	–0.28 ± 0.07	–1.30 ± 0.26	–0.78 ± 0.09	–0.63 ± 0.05	–0.34 ± 0.04	<0.001	–
CON 2 <sup>b</sup> mean ± SD	Max	0.29 ± 0.10	1.30 ± 0.32	0.58 ± 0.11	0.49 ± 0.06	0.30 ± 0.05	<0.001	2 = 8
	Min	–0.30 ± 0.09	–1.30 ± 0.26	–0.78 ± 0.09	–0.63 ± 0.05	–0.34 ± 0.04	<0.001	2 = 8
CON 3 <sup>c</sup> mean ± SD	Max	0.30 ± 0.06	1.30 ± 0.32	0.58 ± 0.11	0.49 ± 0.06	0.30 ± 0.05	<0.001	3 = 8
	Min	–0.21 ± 0.05	–1.30 ± 0.26	–0.78 ± 0.09	–0.63 ± 0.05	–0.34 ± 0.04	<0.001	–
CON 4 <sup>d</sup> mean ± SD	Max	0.20 ± 0.04	1.30 ± 0.32	0.58 ± 0.11	0.49 ± 0.06	0.30 ± 0.05	<0.001	–
	Min	–0.22 ± 0.03	–1.30 ± 0.26	–0.78 ± 0.09	–0.63 ± 0.05	–0.34 ± 0.04	<0.001	–

Indicates no significant difference from Tukey’s post hoc ( $p > 0.05$ ).

<sup>a</sup> CON 1: control 1 phantom.

<sup>b</sup> CON 2: control 2 phantom.

<sup>c</sup> CON 3: control 3 phantom.

<sup>d</sup> CON 4: control 4 phantom.

<sup>e</sup> PDMS A: polydimethylsiloxane A phantom.

<sup>f</sup> PDMS B: polydimethylsiloxane B phantom.

<sup>g</sup> PDMS C: polydimethylsiloxane C phantom.

<sup>h</sup> PDMS D: polydimethylsiloxane D phantom.

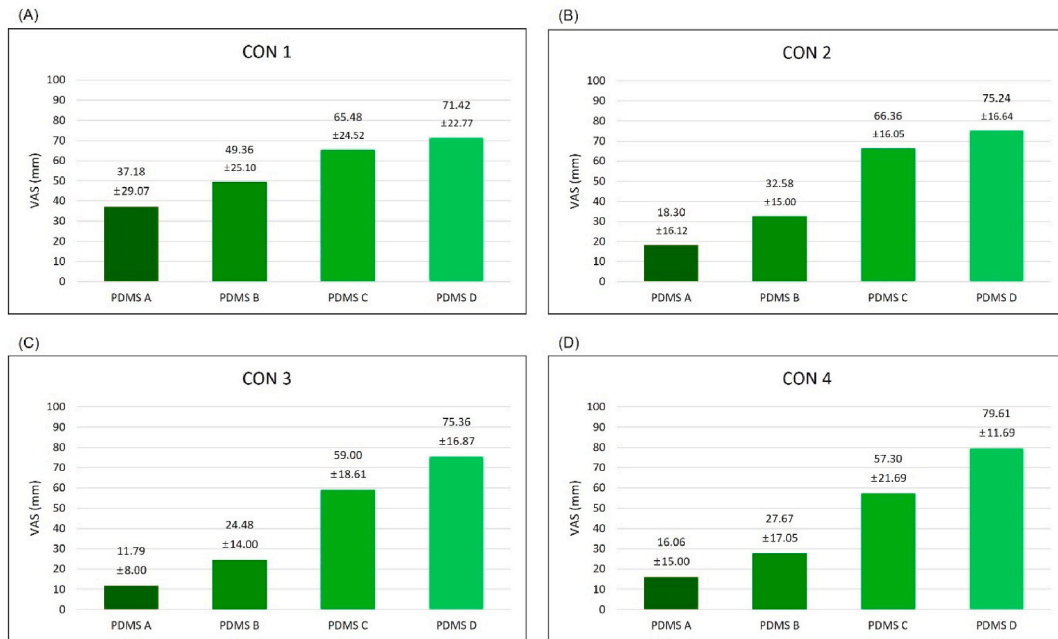


**Fig. 4.** VAS value of similarity to control for each polydimethylsiloxane phantom reported by experts during lifting–thrusting. (CON: control phantom; PDMS: polydimethylsiloxane phantom).

Table 2 shows detailed calculations for the maximum and minimum torque values. There was no significant difference between the groups ( $P$ -value  $>0.05$ ) at maximum torque values. Thus, a post-analysis was not conducted. At minimum torque values, PDMS D was not significantly different from any of the controls, which indicates that PDMS D was most similar to the controls.

The closer the two silicone elastomers of PDMS are to a ratio of 1:4.5, the more the rotational viscosity coefficient of acu-needle sensation delivers a similar sensation as the control phantom as shown in Fig. 6.

Fig. 7(A–D) are the comparison of CON 1 to 4 and PDMS A to D, respectively. In the VAS test results, PDMS D showed the highest score ( $>74.52$  mm) compared to all of the controls in the twirling experiments.

#### 4. Discussion

Acupuncture sensation, which is a key factor in treatment, depends on the intensity of the stimulus [2]. Several studies have shown that the pain and healing effects of acupuncture increase through the manipulation of acu-needles [30–33]. This means that the strength of the stimulus can be controlled through manipulation.

Being able to manipulate an acu-needle is a basic skill of acupuncture practitioners [34]. Performing it well cannot be mastered without practice, yet students tend to be wary of performing this technique on a clinical basis [35,36]. Some studies have demonstrated that students achieve better accuracy when practicing manipulations through repetitive exercises [35,37]. When necessary, students are trained using a tissue-mimicking phantom.

Silicone can be used as a tissue-mimicking phantom [11] due to its inert, nontoxic, noncombustible, and biocompatible properties [38,39]. It is used in medicine as a tissue-mimicking phantom to experience the insertion motion of trocar [13], to mimic breast tissue for education [40], and to measure the ophthalmic tomography system [41].

Often used in biomedical devices, PDMS is characterized by its durability, stability, and ability to be molding into customized shapes. Among the various types of PDMS, this study selected RTV products that can be produced at room temperature to supplement homogeneity and persistence, which were the limitations of the pre-study tissue-mimicking phantoms [18].

Other studies have focused on the surface roughness of PDMS phantoms [42], as well as the nanoindentation and tensile testing properties [43,44] of the material. It is a set of indicators that represents the characteristics of PDMS but not the interactions with other objects. To measure the forces generated by interactions between acu-needle and phantom, force and coefficients were used to assess internal factors.

Furthermore, the control groups were selected to reflect the fact that acupuncture treatment takes place on various parts of the human body. The controls were divided into four parts according to the area of the body represented by each control group. In particular, CON 1, CON 2, and CON 3 consisted mainly of muscle parts, and CON 4 consisted mainly of fatty parts.

Acupuncture's lifting–thrusting method is a linear motion that was analyzed using the modified Karnopp friction model, which was also described in the studies of Son et al. [5] and Okamura et al. [27]. The dynamic and static friction coefficients calculated using this model were used to analyze and compare the linear motion of acupuncture by segmenting it [27]. The dynamic friction coefficient

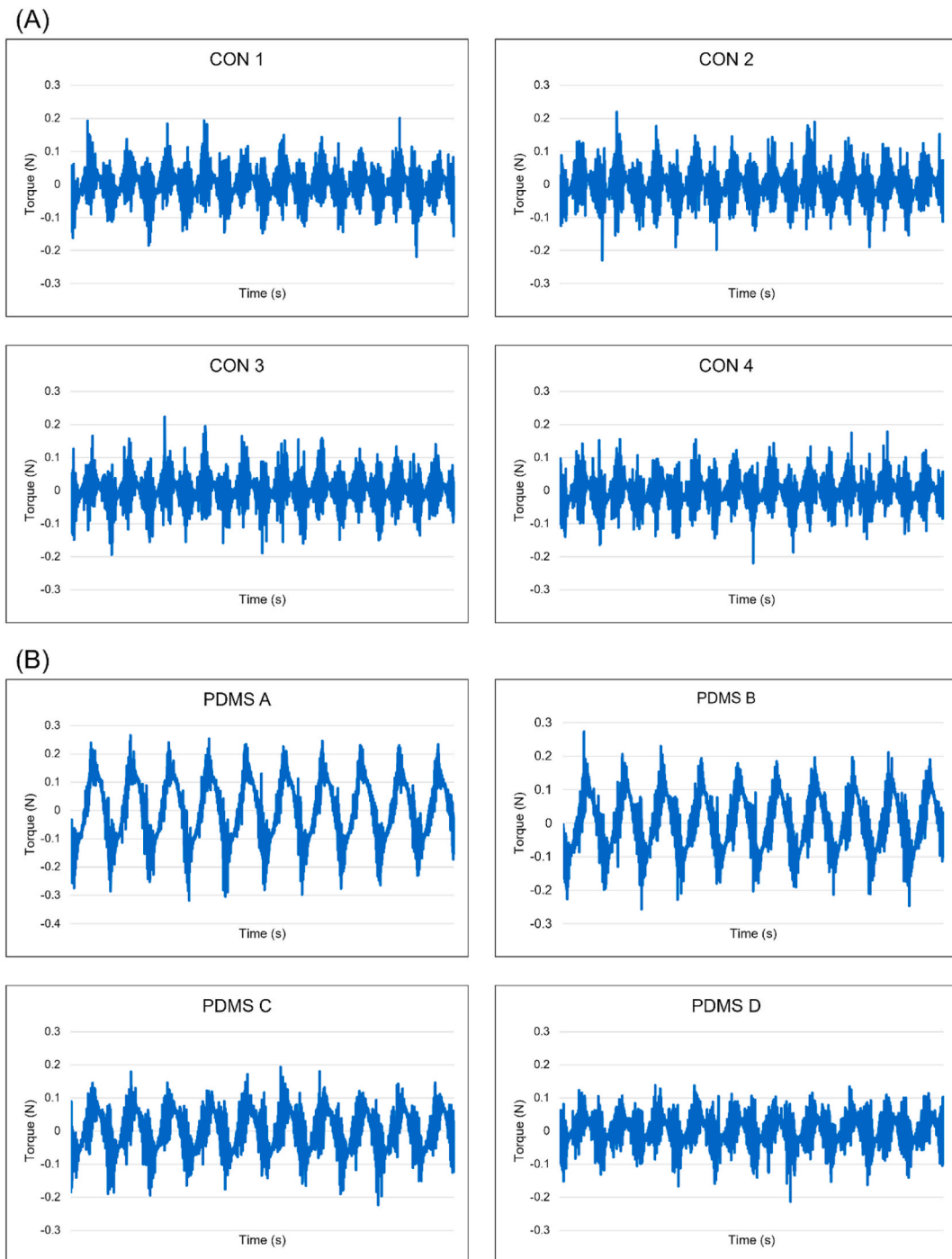


**Fig. 5.** Change in torque over time for control phantoms (A) and polydimethylsiloxane phantoms (B) during rotation-twirling (CON: control phantom; PDMS: polydimethylsiloxane phantom).

reflects the friction phenomenon that occurs when the acu-needle moves in one direction. The dynamic friction is a stiffness that is constantly felt when moving, and is considered an important factor when delivering acupuncture sensation. As mentioned in Son et al. [5]'s study, the positive friction coefficient ( $C_p$ ) generated during lifting-thrusting is an important factor for quantification and comparison to evaluate the suitability of phantom. The static friction coefficient reflects the friction phenomenon that occurs in the section where the direction of the acu-needle changes. The viscosity coefficient has a smaller impact than the dynamic friction coefficient, so it is not expected to have a significant impact unless the speed of insertion of the acu-needle is extremely fast. The twirling

**Table 2**  
Torque of the twirling experiments for Control and Polydimethylsiloxane phantoms.

	(N)					ANOVA p-value	Tukey's HSD	
			PDMS A <sup>a</sup>	PDMS B <sup>f</sup>	PDMS C <sup>g</sup>			PDMS D <sup>h</sup>
			mean ± SD	mean ± SD	mean ± SD			mean ± SD
CON 1 <sup>a</sup> mean ± SD	Max	0.58 ± 0.16	0.56 ± 0.13	0.55 ± 0.15	0.55 ± 0.15	0.53 ± 0.13	0.10	
	Min	-0.59 ± 0.18	-0.68 ± 0.17	-0.64 ± 0.20	-0.61 ± 0.18	-0.59 ± 0.18	<0.001	1 = 6 1 = 7 1 = 8
CON 2 <sup>b</sup> mean ± SD	Max	0.58 ± 0.18	0.56 ± 0.13	0.55 ± 0.15	0.55 ± 0.15	0.53 ± 0.13	0.16	
	Min	-0.59 ± 0.17	-0.68 ± 0.17	-0.64 ± 0.20	-0.61 ± 0.18	-0.59 ± 0.18	0.001	2 = 6 2 = 7 2 = 8
CON 3 <sup>c</sup> mean ± SD	Max	0.58 ± 0.15	0.56 ± 0.13	0.55 ± 0.15	0.55 ± 0.15	0.53 ± 0.13	0.08	
	Min	-0.57 ± 0.17	-0.68 ± 0.17	-0.64 ± 0.20	-0.61 ± 0.18	-0.59 ± 0.18	<0.001	3 = 7 3 = 8
CON 4 <sup>d</sup> mean ± SD	Max	0.56 ± 0.14	0.56 ± 0.13	0.55 ± 0.15	0.55 ± 0.15	0.53 ± 0.13	0.35	
	Min	-0.56 ± 0.18	-0.68 ± 0.17	-0.64 ± 0.20	-0.61 ± 0.18	-0.59 ± 0.18	<0.001	4 = 7 4 = 8

Indicates no significant difference from Tukey's post hoc (p > 0.05).

- <sup>a</sup> CON 1: control 1 phantom.
- <sup>b</sup> CON 2: control 2 phantom.
- <sup>c</sup> CON 3: control 3 phantom.
- <sup>d</sup> CON 4: control 4 phantom.
- <sup>e</sup> PDMS A: polydimethylsiloxane A phantom.
- <sup>f</sup> PDMS B: polydimethylsiloxane B phantom.
- <sup>g</sup> PDMS C: polydimethylsiloxane C phantom.
- <sup>h</sup> PDMS D: polydimethylsiloxane D phantom.

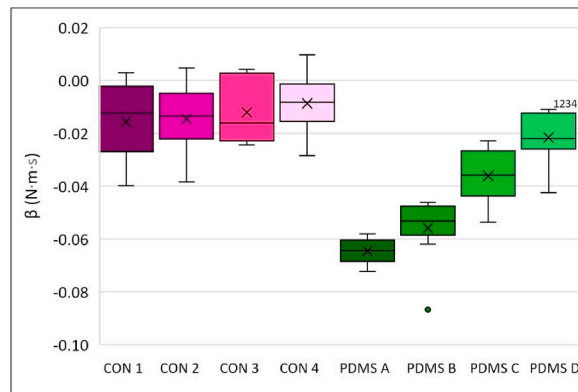


**Fig. 6.** Viscosity coefficients for each phantom during twirling with the numbers referring to CON that do not differ significantly from PDMS (CON: control phantom; PDMS: polydimethylsiloxane phantom).

method is a rotary motion, and its viscosity coefficient has been calculated from the torque value according to the method used by Reed et al. [28] and as an indicator for evaluating phantoms during rotary motion in Han et al. [4]. The maximum and minimum value were calculated from the force generated during a single exercise, and it is thought that these can be altered by the characteristics of the phantom and acu-needle [29]. In this study, when an acu-needle of the same condition was used, the maximum and minimum values were used as variables that could be influenced by the characteristics of the phantom.

The experiment revealed that, of the four selected tissue-mimicking phantoms, PDMS D was statistically similar to CON 2 in terms of  $C_p$  and the maximum and minimum friction force values, which means that PDMS D can be used as a phantom to practice lifting–thrusting techniques on behalf of CON 2. Analysis of the torque generated by the interaction between the acu-needle and phantom showed that PDMS D was most similar to the controls.

According to the VAS of Korean medicine doctors comparing the sensations of the acu-needle for the control and PDMS groups, PDMS D is considered to be the most similar to each of the control groups by more than 71.42 points.

The overall results of the experiment revealed that PDMS D showed the most similar value to the controls, and therefore is considered to be the most suitable substitute for CON 2, which was porcine muscle. Since acupuncture points used in clinical practice are located in the muscles, PDMS D is thought to be meaningful for practicing acupuncture on muscle areas. Given that we were able to find matching phantoms based on multiple conditions, the phantom used in this study is recommended for use as a tissue-mimicking phantom in future research. It will be helpful to develop a phantom replacement for fat and phantoms that depend on the muscle layer.

This study tried to present new tissue-mimicking phantoms for acupuncture manipulations by complementing the weaknesses of existing tissue-mimicking phantoms, such as the sustainability and biocompatibility of PDMS. It is meaningful that PDMS was selected as a tissue-mimicking phantom and has been studied quantitatively in the acupuncture field. According to this study, PDMS could be

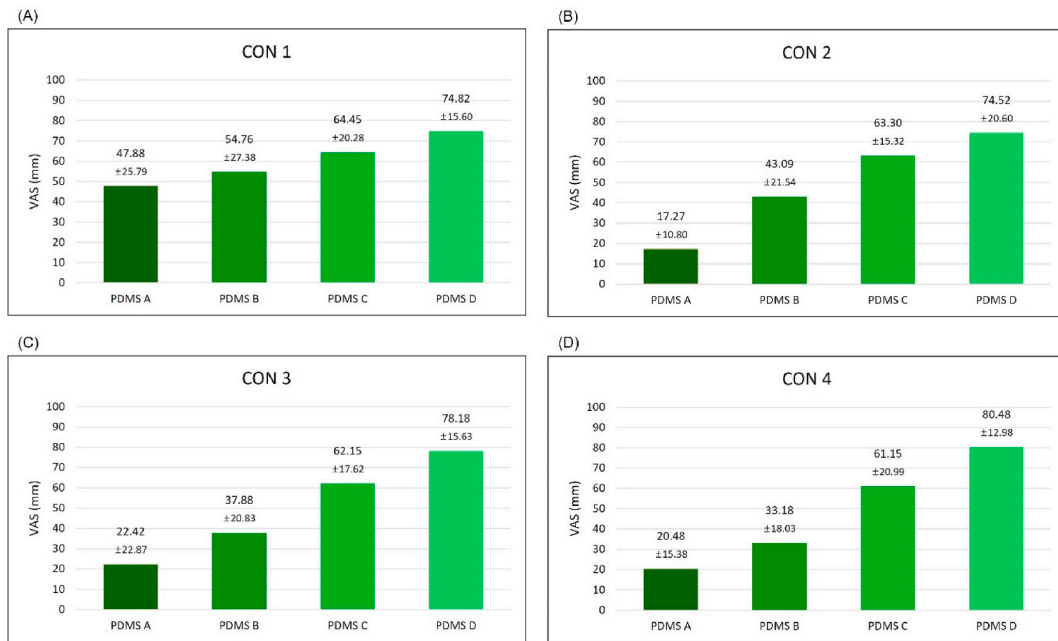


**Fig. 7.** VAS value of similarity to control for each polydimethylsiloxane phantom reported by experts during rotating–twirling. (CON: control phantom; PDMS: polydimethylsiloxane phantom).

used as a platform for learning acupuncture manipulation. Additionally, the force generated by the interaction of the acu-needle with tissue was analyzed in comparison with acupuncture manipulations based on friction and viscosity coefficients and was analyzed with objective numerical values when the manipulations were enforced. As a result, both friction and viscosity coefficients may be presented as tools for objectively evaluating acupuncture sensations as a means to judge the suitability of a tissue-mimicking phantom.

However, there are many different kinds of PDMS available, but this experiment was limited to just one type. It was also limited by an inability to analyze various acupuncture manipulations, and the utilization of porcine tissue instead of human tissue as a control group required carrying out the same movement repeatedly. Since it is porcine tissue that is widely used as a substitute for human tissue [20–22], it appears plausible to substitute the phantom as done in this study; however, further studies on different movements are required. Since movements occur continuously, it is believed that analyzing continuous interactions will be necessary in the future, rather than focusing solely on the analysis of individual moments of power.

In the future, a range of manipulations should be used to determine the suitability of a tissue-mimicking phantom, and in addition to the phantoms used in this study, a comparison of several phantoms will lead to the development of one that can be used to refine the techniques of acupuncture practitioners. Further research is needed to find an appropriate phantom, which involves comparing it with various parts of tissue and potentially altering the mixing ratio or diversifying the types of PDMS used. Importantly, the development of phantoms that can reflect different human tissues will improve the overall experience gained from acupuncture trials.

#### Data availability statement

All data analyzed in this study are available upon request from the corresponding author.

#### Sources of support in the form of grant

This work was supported by the National Research Foundation of Korea (NRF) grant funded by the Korea government (MSIT). (No. 2019R1A2C1086643)

#### CRediT authorship contribution statement

**Yeonsun Lee:** Writing – review & editing, Writing – original draft, Validation, Software, Resources, Methodology, Investigation, Formal analysis, Data curation, Conceptualization. **Hyosang Lee:** Writing – review & editing, Software, Methodology, Formal analysis. **Eun Jung Kim:** Visualization, Resources. **Seung Deok Lee:** Software, Methodology, Conceptualization. **Chan Yung Jung:** Writing – review & editing, Validation, Supervision, Project administration, Methodology, Conceptualization.

## Declaration of competing interest

The authors declare the following financial interests/personal relationships which may be considered as potential competing interests:

Chan Yung Jung reports financial support was provided by National Research Foundation of Korea. If there are other authors, they declare that they have no known competing financial interests or personal relationships that could have appeared to influence the work reported in this paper.

## Acknowledgements

This work was supported by the National Research Foundation of Korea(NRF) grant funded by the Korea government(MSIT). (No. 2019R1A2C1086643)

## References

- [1] R. Lebert, Medical acupuncture., Evidence-Based Massage Therapy : A Guide for Clinical Practice (2020) 90–98.
- [2] Y.J. Choi, et al., Does the effect of acupuncture depend on needling sensation and manipulation? *Compl. Ther. Med.* 21 (3) (2013) 207–214.
- [3] C.J. Zaslowski, et al., The impact of site specificity and needle manipulation on changes to pain pressure threshold following manual acupuncture: a controlled study, *Compl. Ther. Med.* 11 (1) (2003) 11–21.
- [4] Y.J. Han, et al., Comparative study of needle sensations in ST and 6 models with quantifying measurement system, *J Korean Acupunct Moxibustion Soc* 30 (5) (2013) 87–94.
- [5] Y.N. Son, et al., Friction coefficient for the quantification of needle grasp in the lifting-thrusting method, *Int. J. Precis. Eng. Manuf.* 15 (7) (2014) 1429–1434.
- [6] J.F. Nitsche, et al., Effectiveness of labor cervical examination simulation in medical student education, *Obstet. Gynecol.* 126 (Suppl 4) (2015) 13s–20s.
- [7] R. Öpik, et al., Development of high fidelity liver and kidney phantom organs for use with robotic surgical systems, in: 2012 4th IEEE RAS & EMBS International Conference on Biomedical Robotics and Biomechatronics (BioRob), IEEE, 2012.
- [8] S.L. Vieira, et al., Paraffin-gel tissue-mimicking material for ultrasound-guided needle biopsy phantom, *Ultrasound Med. Biol.* 39 (12) (2013) 2477–2484.
- [9] S.W. Allison, et al., In vivo X-Ray excited optical luminescence from phosphor-doped aerogel and Sylgard 184 composites, *Radiat. Phys. Chem.* 135 (2017) 88–93.
- [10] L. Bernardi, et al., On the cyclic deformation behavior, fracture properties and cytotoxicity of silicone-based elastomers for biomedical applications, *Polym. Test.* 60 (2017) 117–123.
- [11] P. Li, Z. Yang, S. Jiang, Tissue mimicking materials in image-guided needle-based interventions: a review, *Mater Sci Eng C* 93 (2018) 1116–1131.
- [12] I.S. Lee, et al., Haptic simulation for acupuncture needle manipulation, *J. Alternative Compl. Med.* 20 (8) (2014) 654–660.
- [13] Y. Wang, et al., Silicone-based tissue-mimicking phantom for needle insertion simulation, *J. Med. Dev. Trans. ASME* 8 (2) (2014).
- [14] N. Abolhassani, R. Patel, M. Moallem, Experimental study of robotic needle insertion in soft tissue, in: International Congress Series, Elsevier, 2004.
- [15] J.E. Jang, et al., Trends in acupuncture training research: focus on practical phantom models, *J Acupunct Res* 39 (2) (2022) 77–88.
- [16] T. Liu, et al., Application research of neural network in acupuncture training system, *Comput. Technol. Autom.* 39 (2020) 102–107.
- [17] R.L. Cai, L. Hu, P. Wang, Z.J. Wu, W.H. Chen, Y.F. Meng, Research and practice on the construction of simulative training platform of acupuncture for the acupoints on the specific sites of human body, *Zhongguo Zhen Jiu* (33) (2013) 67–69.
- [18] Y.S. Lee, et al., A study on the quantitative characteristics of needle force on the acupuncture practical model, *Korean J Acupunct* 35 (3) (2018) 149–158.
- [19] Z. Brounstein, et al., Long-term thermal aging of modified sylgard 184 formulations, *Polymers* 13 (18) (2021) 3125.
- [20] G. Hocking, S. Hebard, C.H. Mitchell, A review of the benefits and pitfalls of phantoms in ultrasound-guided regional anesthesia, *Reg. Anesth. Pain Med.* 36 (2) (2011) 162–170.
- [21] P. Mignon, P. Poignet, J. Troccaz, Automatic robotic steering of flexible needles from 3D ultrasound images in phantoms and ex vivo biological tissue, *Ann. Biomed. Eng.* 46 (2018) 1385–1396.
- [22] P.J. Swaney, et al., A flexure-based steerable needle: high curvature with reduced tissue damage, *IEEE Trans. Biomed. Eng.* 60 (4) (2012) 906–909.
- [23] World Health Organization, WHO International Standard Terminologies on Traditional Medicine in the Western Pacific Region, 2007.
- [24] H.R. Kang, et al., Review of acupuncture manipulation in clinical trials, *Acupunct* 33 (3) (2016) 129–144.
- [25] J. Li, et al., Perceptual motor features of expert acupuncture lifting-thrusting skills, *Acupunct. Med.* 31 (2) (2013) 172–177.
- [26] Y.J. Han, et al., Quantification of the parameters of twisting–rotating acupuncture manipulation using a needle force measurement system, *Integr Med Res* 4 (2) (2015) 57–65.
- [27] A.M. Okamura, C. Simone, M.D. O’leary, Force modeling for needle insertion into soft tissue, *IEEE Trans. Biomed. Eng.* 51 (10) (2004) 1707–1716.
- [28] K.B. Reed, A.M. Okamura, N.J. Cowan, Modeling and control of needles with torsional friction, *IEEE Trans. Biomed. Eng.* 56 (12) (2009) 2905–2916.
- [29] Y.S. Lee, et al., Quantitative comparison of acupuncture needle force generation according to diameter, *J Acupunct Res* 35 (4) (2018) 238–243.
- [30] S.R. Min, et al., Local changes in microcirculation and the analgesic effects of acupuncture: a laser Doppler perfusion imaging study, *J. Alternative Compl. Med.* 21 (1) (2015) 46–52.
- [31] S.Y. Liu, et al., Acupuncture stimulation improves balance function in stroke patients: a single-blinded controlled, randomized study, *Am. J. Chin. Med.* 37 (3) (2009) 483–494.
- [32] S.B. Xu, et al., Effectiveness of strengthened stimulation during acupuncture for the treatment of Bell palsy: a randomized controlled trial, *CMAJ (Can. Med. Assoc. J.)* 185 (6) (2013) 473–478.
- [33] Y. Kong, et al., Effects of the lifting manipulation of scalp acupuncture for raising myodynamia of the affected limbs in hemiplegic patients due to cerebral thrombosis, *J Tradit Chinese Med* 25 (4) (2005) 256–259.
- [34] H. Park, Clinical skills assessment in Korean medical licensing examination, *Korean Korean J Med Educ* 20 (4) (2008) 309–312.
- [35] I.S. Lee, et al., Evaluation of phantom-based education system for acupuncture manipulation, *PLoS One* 10 (2) (2015) e0117992.
- [36] Y. Seo, et al., Motion patterns in acupuncture needle manipulation, *Acupunct. Med.* 32 (5) (2014) 394–399.
- [37] W.M. Jung, et al., Sensorimotor learning of acupuncture needle manipulation using visual feedback, *PLoS One* 10 (9) (2015) e0139340.
- [38] J.C. McDonald, et al., Fabrication of microfluidic systems in poly (dimethylsiloxane), *Electrophor An Int J* 21 (1) (2000) 27–40.
- [39] S. Halldorsson, et al., Advantages and challenges of microfluidic cell culture in polydimethylsiloxane devices, *Biosens. Bioelectron.* 63 (2015) 218–231.
- [40] B. Ustbas, et al., Silicone-based composite materials simulate breast tissue to be used as ultrasonography training phantoms, *Ultrasonics* 88 (2018) 9–15.
- [41] J. Baxi, et al., Retina-simulating phantom for optical coherence tomography, *J. Biomed. Opt.* 19 (2) (2013) 021106.
- [42] R.N. Palchesko, et al., Development of polydimethylsiloxane substrates with tunable elastic modulus to study cell mechanobiology in muscle and nerve, *PLoS One* 7 (12) (2012) e51499.
- [43] A. Mata, A.J. Fleischman, S. Roy, Characterization of polydimethylsiloxane (PDMS) properties for biomedical micro/nanosystems, *Biomed. Microdevices* 7 (4) (2005) 281–293.
- [44] C.M. Buffinton, et al., Comparison of mechanical testing methods for biomaterials: pipette aspiration, nanoindentation, and macroscale testing, *J. Mech. Behav. Biomed. Mater.* 51 (2015) 367–379.